ASEAN
Journal of Scientific and Technological Reports
Online ISSN:2773-8752

Research article

Service Life Prediction of Natural Rubber/Reclaimed Rubber Blends through Thermogravimetric Analysis

Sutiwat Thumrat[1], Weerawut Naebpetch[2], Sitisaiyidah Saiwari[1], and Nabil Hayeemasae[1*]

[1] Faculty of Science and Technology, Prince of Songkla University, Pattani Campus, Pattani, 94000, Thailand
[2] Faculty of Engineering, Thaksin University, Phatthalung Campus, Phatthalung, 93210, Thailand
* Correspondence: nabil.h@psu.ac.th

Citation:
Thumrat, S.; Naebpetch, W.; Saiwari, S.; Hayeemasae, N. Service Life Prediction of Natural Rubber/Reclaimed Rubber Blends through Thermogravimetric Analysis. *ASEAN J. Sci. Tech. Report.* **2026**, *29*(3), e261676. https://doi.org/10.55164/ajstr.v29i3.261676.

Article history:
Received: October 1, 2025
Revised: January 28, 2026
Accepted: February 5, 2026
Available online: February 28, 2026

Abstract: The rubber products containing reclaimed rubber may have influenced the service life due to their prior degradation history. However, not many rubber compounders know their service life until they have used it for a certain period. This study breaks this barrier by proposing a simple, cost-effective prediction method based on thermogravimetric analysis (TGA). It focused on blends of Natural Rubber (NR) and Reclaimed Rubber (RR) at various blending ratios. The Ozawa–Flynn–Wall (OFW) Method was applied to the TGA outputs. The results showed that NR/RR blends at all ratios had slightly lower lifetimes than virgin NR over the temperature range of 30-600 °C. When considering a service temperature of 70 °C, the use of RR at 50 phr could reduce the service life from 195 years to 2.01 years. This indicates that the addition of RR may severely affect the service life of the products. The results of this study are useful information for rubber compounders when using RR in their formulations.

Keywords: Lifetime prediction; service life; reclaimed rubber; natural rubber; thermogravimetric analysis

1. Introduction

The problem of waste from worn-out rubber items like tires is growing rapidly, with around 1 billion tires discarded each year. It is anticipated that this figure will increase to 1.2 billion by the year 2030 [1]. Disposing of these rubber products by incineration or landfilling causes significant environmental pollution in the air and soil, as vulcanized rubber is non-biodegradable and not easily recyclable [2]. Accumulated tires are prone to catching fire, causing long-lasting environmental damage and air pollution [3,4]. A significant portion of waste tires is disposed of illegally, contributing to environmental degradation [5]. This poses a significant difficulty in eco-friendly rubber waste management. A potential approach is the creation of reclaimed rubber (RR), in which old vulcanized rubber is heated and treated with chemicals to break molecular chains, enabling it to undergo re-vulcanization. Nonetheless, reclaimed rubber usually shows reduced mechanical properties, such as tensile strength and elongation at break, compared to virgin rubber because the reclamation process randomly cuts chains, which may affect the main chain and result in a lower molecular weight [6, 7, 8]. But at the same time, researchers have continuously sought to increase the efficiency of RR use by applying advanced recycling methods, such as ultrasonic grinding [9], microbial devulcanization [10], and microwave devulcanization [11], to name a few. However, these methods have

not been widely scaled up at the industrial level, so the resulting performance decrease limits the potential use of recycled rubber in demanding applications such as tires or high-quality rubber products.

As mentioned, rubber products containing RR may have a shorter service life due to their inherent properties. Not many rubber manufacturers know their service life until they observe the products after a certain period of use. Therefore, predicting the lifetime of rubber products containing RR is challenging and essential for accurately utilizing recovered rubber to address these constraints. The Arrhenius equation is commonly used to predict product lifetime by relating degradation mechanisms to temperature, as reaction rates increase with temperature [12]. This study applied this equation to the outputs from Thermogravimetric Analysis (TGA). The reliability of TGA-based kinetics for lifetime prediction has been validated in various material systems. For instance, Núñez et al. [13] successfully utilized this technique for epoxy resin systems, while Viorel et al. [14] applied it to catalytic materials. In the context of rubber, Ngudsuntear et al. [15] employed TGA kinetics for hydrogenated epoxidized natural rubber (HENR), and Ahn et al. [16] demonstrated strong agreement between TGA predictions and accelerated aging tests for automotive rubber composites. These applications are grounded in the foundational theory established by Toop [17], confirming that non-isothermal TGA is a robust tool for estimating material longevity. To date, there has been limited discussion of the lifetime prediction of NR/RR blends, and it remains unclear whether variations in RR loading have a positive or negative effect on the long-term durability of the final product. This study offers a simple, cost-effective method for predicting the service life of materials. This is unlike other experiments, which require more time and a larger budget. TGA can be performed for a short time, during which the data obtained from its outputs is sufficient to estimate the lifetime. The findings from this research will serve as a foundation for the development of RR-based rubber products.

2. Materials and Methods

2.1 Materials

This study primarily utilized natural rubber (NR) and reclaimed rubber (RR). The NR was of RSS3 grade, prepared in accordance with Thai industrial standards. Yupphadirubber Part., Ltd manufactured the RSS3. The RR was supplied by Union Commercial Development Co., Ltd., Bangkok, Thailand. The RR used was a UCD-105 grade in bulk form (slabs), with a thermo-mechanical process in the presence of a reclaiming agent. According to TGA analysis, RR contained 56.92% rubber hydrocarbon, 10.54% oil, 27.39% carbon black, and 5.15% inorganic matter. Other compounding ingredients, such as Zinc oxide, were purchased from Thai-Lysaght Co., Ltd., Phra Nakhon Si Ayutthaya, Thailand. Stearic acid was purchased by Permata Group Pte. Ltd., Sumatra Utara, Indonesia. Paraffin wax and Paraffinic oil were purchased by H&R Chem Pharm (Thailand) Co., Ltd., Bangkok, Thailand. $CaCO_3$ was purchased by Phatthana Chemical Co., Ltd., Songkhla, Thailand, with an average particle size of 45-50 μm. Carbon black (N550) grade was purchased by Thai Tokai Carbon Product Co., Ltd., Bangkok, Thailand, having a primary particle size of approximately 40–60 nm. N-Cyclohexyl-2-Benzothiazol Sulfenamide (CBS) was purchased by Kawaguchi, Co., Ltd., Tokyo, Japan. Sulfur was purchased by Siam Chemical, Co., Ltd., Bangkok, Thailand. All these materials and chemicals were used as received.

2.2 Preparation of rubber blends

Table 1 shows the blending formulation for NR and RR. The blending ratios were 100/0, 90/10, 70/30, and 50/50 phr/phr. Later, these blending ratios were abbreviated as RR0, RR10, RR30, and RR50, respectively. The content of hydrocarbon rubber, carbon black, and other additives in RR was analyzed using Thermogravimetric analysis (TGA) in accordance with ASTM D6370-99. These data were used to adjust the amounts of virgin NR and fillers in the formulations to ensure that the total content of rubber hydrocarbon and fillers remained consistent across all blends and was comparable to the control (RR0). The entire amount of ingredients, except for CBS and sulfur, was compounded in a 50-L dispersion kneader at a controlled temperature of 75-80 °C for 60 minutes. Subsequently, the compounds were passed through the two-roll mill to add the CBS and sulfur. Finally, the resultant compounds were compression-molded at 150 °C. The time consumed was based on the curing times measured by a moving-die rheometer (MDR), as described in the

following section. Notably, these formulations were derived from a commercial rubber wheel stopper compound, which requires high filler loading for dimensional stability and cost-effectiveness under static loading conditions.

Table 1. Compounding ingredients for preparing NR/RR blends.

Material	Role	Amount (phr)			
		RR0	**RR10**	**RR30**	**RR50**
Natural rubber	Rubber matrix	100	90	70	50
Reclaimed rubber	Rubber matrix	0	10	30	50
Zinc Oxide	Activator	3	3	3	3
Stearic acid	Activator	1	1	1	1
Paraffin wax	Antiozonant	2	2	2	2
$CaCO_3$	Filler	100	100	100	100
N550	Filler	40	40	40	40
Paraffinic oil	Plasticizer	15	15	15	15
CBS	Accelerator	1.5	1.5	1.5	1.5
Sulfur	Vulcanizing agent	1	1	1	1

Note: The amounts of Paraffinic oil, Carbon Black (N550), and Calcium Carbonate ($CaCO_3$) added were adjusted based on the composition of RR to maintain a constant total filler loading.

2.3 Measurement of Mooney viscosity

The Mooney viscosity of the rubber blends was determined using a Mooney viscometer (ML1+4, 100 °C) in accordance with ASTM D1646. The tests were conducted on three samples to measure the Mooney viscosity of the rubber blends before vulcanization**.**

2.4 Measurement of Curing Characteristics

The vulcanization properties of the rubber blends were analyzed using a moving die rheometer (MDR) at 150 °C for 30 minutes, in accordance with ASTM D5289. To find Scorch time (t_{s1}), Cure time (t_{c90}), Maximum torque (M_H), Minimum torque (M_L), Torque difference ($M_H - M_L$), and Cure rate index (CRI).

2.5 Measurement of mechanical properties

Tensile properties were measured using a Universal Testing Machine in accordance with ASTM D412. Test specimens were fabricated in five replicates, each having a gage length of 25 mm. The crosshead velocity was established at 500 mm/min. The tensile strength and elongation at break were recorded for each specimen. The tear strength was evaluated in accordance with ASTM D624 (Die C), utilizing an angular-shaped test specimen. The examination was performed at a crosshead velocity of 500 mm/min with a force of 500 N. The hardness was assessed utilizing an Automatic Rubber Hardness Tester fitted with a Shore A durometer. Test specimens were fabricated as square samples measuring 6 x 6 cm and 0.9 cm in thickness, in accordance with ASTM D2240. To evaluate the durability of the rubber blends, aging tests were conducted under two conditions: thermal aging and oil-swollen aging. For thermal aging, dumbbell-shaped specimens were placed in a hot-air oven at 100 °C for 7 days (168 h), in accordance with ASTM D573. For oil-swelling aging, the specimens were immersed in SAE 5W-30 oil at 100 °C for 7 days (168 h) in accordance with ASTM D471. After aging, the samples were allowed to rest at room temperature for at least 24 h before testing for mechanical properties.

2.6 Thermogravimetric analysis

A Perkin-Elmer Pyris 6 TGA analyzer was used to perform a thermogravimetric analysis (TGA) on samples weighing approximately 9.263 mg. The samples were heated at 5, 10, 15, and 20 °C/min in a nitrogen flow while being scanned from 30 °C to 600 °C.

2.7 Thermal Kinetics Analysis

TGA is essential for predicting material lifetime by modeling degradation processes. These models help analyze phase transitions and chemical reactions under heat, determining key kinetic parameters such as

activation energy (E_a), Arrhenius pre-exponential factor (A), and reaction order (n). For non-isothermal conditions, the reaction rate constant (k) is temperature-dependent and follows the Arrhenius equation [18]. The fundamental kinetic relationship of the degradation process is described in Equation (1):

$$\frac{d\alpha}{dt} = k(T) \cdot f(\alpha) \tag{1}$$

Where $k(T)$ is the temperature-dependent reaction rate constant, and $f(\alpha)$ represents the reaction model.

The degradation of polymers is measured by the decline in their properties, where the degradation rate depends on temperature. Higher temperatures accelerate the reaction rate and increase the rate constant (k) according to the Arrhenius equation, [18] as described in Equation (2):

$$k(T) = A \cdot e^{-\frac{E_a}{RT}} \tag{2}$$

Where: A is Arrhenius pre-exponential factor, E_a is Activation energy (J/mol), R is Gas constant (8.314 J/mol/K), T is Absolute temperature (K).

To eliminate the time dependence in Equation (1), which relies on temperature (T) and conversion rate (α), the equation can be transformed by dividing the differential form by the heating rate [18]. This results in Equation (3):

$$\frac{d\alpha}{dT} = \frac{A}{\beta} \cdot e^{-\frac{E_a}{RT}} \cdot f(\alpha) \tag{3}$$

Where β is the heating rate (°C/min).

The Friedman's Method (FRD) is an isoconversion differential technique used to analyze the kinetic parameters of thermal degradation. It can be derived by applying the natural logarithm (ln) to both sides of Equation (1), [15,16] leading to the simplified expression shown in Equation (4).

$$ln\left(\frac{d\alpha}{dT}\right) = constant \cdot -\frac{E_a}{RT} \tag{4}$$

The Kissinger–Akahira–Sunose (KAS) method is an isoconversion technique used to evaluate the kinetic parameters of thermal degradation. It can be calculated using the Coats−Redfern equation [15,16] as expressed in Equation (5).

$$ln\left(\frac{\beta}{T^2}\right) = constant \cdot -\frac{E_a}{RT} \tag{5}$$

The Ozawa–Flynn–Wall (OFW) method is an integral isoconversion technique used to determine the activation energy (E_a). This method analyzes the relationship between the heating rate (β) and temperature (T) at a constant conversion rate. By plotting $ln(\beta)$ against $1000/T$, the slope of the resulting straight line corresponds to E_a/R [15,16]. The mathematical expression for this relationship is shown in Equation (6):

$$ln(\beta) = \ln\left(\frac{AE_a}{f(a)R}\right) - 5.331 - 1.052\frac{E_a}{R}\left(\frac{1}{T}\right) \tag{6}$$

By combining Toop's equation with the activation energy (E_a) obtained from the OFW method, the lifetime of the material can be predicted [15,16,17]. The relationship is expressed in Equation (7):

$$\ln(t_f) = \frac{E_a}{RT_f} + \ln\left(\frac{E_a}{\beta R} \cdot P(x_f)\right) \quad (7)$$

Where t_f is Thermal life (min), T_f is Operating temperature (K), $P(x_f)$ is Doyle approximation integral.

3. Results and Discussion

3.1 Mooney viscosity

Figure 1 shows the Mooney viscosity of NR/RR blends. To characterize the starting material, the viscosity of neat reclaimed rubber (RR100) was measured at 21.80 MU. As observed, the viscosity of the blends decreases with increasing RR content. It is well known that the reclaiming process for RR involves breaking crosslinking bonds to restore the condition as close as possible to the original rubber. However, during the reclaiming process, especially under mechanical force, the main molecular chains are also damaged, so when re-vulcanized, their strength will be reduced accordingly. In addition, in other research, it was found that the phase-separation factors of NR and RR also decreased the Mooney viscosity of the blends compared to pure NR or pure RR [8].

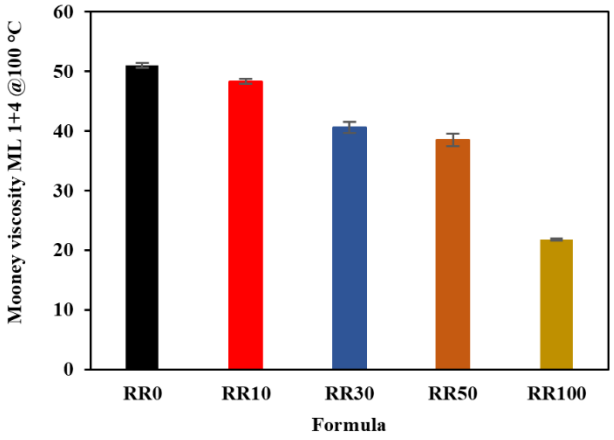

Figure 1. Mooney viscosity of NR/RR blends at ratios of 100/0, 90/10, 70/30, 50/50, and 0/100.

3.2 Curing characteristics

Figure 2 presents the rheometric curves of the NR/RR blends, and the summarized data are listed in Table 2. It can be observed that t_{s1} showed marginal variations across the blends, indicating that the addition of reclaimed rubber did not significantly alter the premature vulcanization safety of the compounds. However, t_{c90} increased slightly, resulting in a lower cure rate as the amount of reclaimed rubber increased. This retardation in curing is attributed to the lower degree of unsaturation (lower carbon-carbon double bond concentration) in reclaimed rubber compared to virgin NR [19]. Since the RR has previously undergone vulcanization and reclaiming, a significant portion of its double bonds has been consumed. Consequently, the depletion of available reactive sites for sulfur crosslinking decreases the overall reaction rate, requiring a longer time to reach the optimal cure state. In addition, as the amount of RR increases, the minimum torque (ML), maximum torque (MH), and delta torque (MH-ML) decrease, indicating a decrease in linkage density due to shortened molecular chains resulting from the reclaiming process [20].

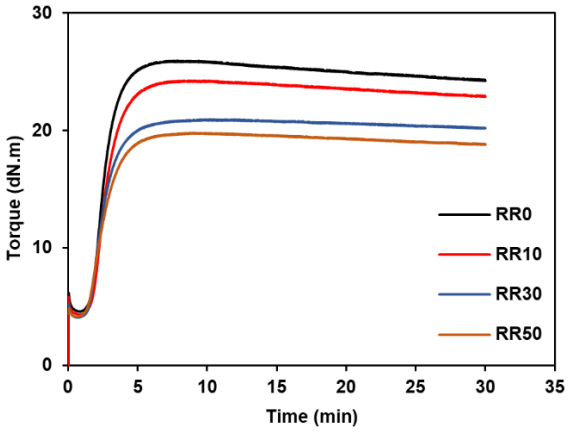

Figure 2. Curing characteristics of NR/RR blends at ratios of 100/0, 90/10, 70/30, and 50/50.

Table 2. Minimum torque (M_L), maximum torque (M_H), torque difference ($M_H - M_L$), and cure rate index (CRI) for NR/RR blends at ratios of 100/0, 90/10, 70/30, and 50/50.

Sample	t_{s1} (min)	t_{c90} (min)	M_H (dN.m)	M_L (dN.m)	M_H-M_L (dN.m)	CRI (min^{-1})
RR0	1.58	4.06	25.95	4.57	21.38	40.34
RR10	1.64	4.39	24.26	4.31	19.95	36.38
RR30	1.49	4.27	20.95	4.08	16.87	35.91
RR50	1.40	4.33	19.80	4.13	15.67	34.07

3.3 Mechanical properties of NR/RR blends

Figures 3 and 4 show the tensile properties, tear strength, and hardness of NR/RR blends. It showed that tensile strength decreased with increasing reclaimed rubber (RR) content. It is widely known that RR was originally cured before undergoing the reclaiming process. So, there was a crosslinking precursor. Such a crosslink precursor can cause catastrophic failure of the sample during stretching, reducing stress transfer. As a result, the tensile strength is reduced. This also affected the elongation at break of the blends (see Figure 3b). The higher RR content eventually reduced the flexibility of the blends. The tensile strength and elongation at break appear to be influenced by the virgin NR. This behavior can be explained by the high strength associated with strain-induced crystallized (SIC) of NR [21]. The ability of NR to undergo SIC decreased with increasing RR content. Furthermore, the tear strength also exhibited the same trend, decreasing with the addition of RR. A similar reason also applies here, as tear strength depends on the SIC of NR. Furthermore, other studies indicate that combinations of NR and RR frequently fail to form a homogenous phase, resulting in inconsistent dispersion within the material [6-8]. This structural inhomogeneity additionally exacerbates the decline of mechanical characteristics. However, Figure 4b shows that the hardness of the blends increased with increasing RR content. The addition of RR to the rubber matrix increased the vulcanizates' stiffness, as hardness is an indicator of material stiffness. As more RR was incorporated into the NR, the flexibility and elasticity of the rubber chains decreased, resulting in greater rigidity and hardness in the rubber vulcanizates.

The properties of the blends after aging are also observed in this study. It was done under normal thermal aging conditions and oil-swollen aging conditions. Both types of thermal aging reduced the overall properties of the blends. The decline in overall mechanical properties can be attributed to oxidation of the polymer, which leads to chain scissions. The breaking of larger molecular chains increased the number of shorter chains, resulting in fewer entanglements and, consequently, a reduction in the mechanical properties. Moreover, the reduction was highest for the thermal aging in oil. The decrease in various properties when immersed in oil is due to NR, which is mainly composed of hydrocarbons, and the RR in this study also has NR as its main component, which is low in polarity. Therefore, when it comes into contact with oil, which is also a hydrocarbon with low polarity, it permeates into the structure, causing the molecular chains to swell and reduce various mechanical properties [15]. To strictly evaluate the durability of the blends, the percentage

retention of tensile strength after aging was calculated and presented in Figure 5. Interestingly, after thermal aging at 100 °C for 7 days, the RR50 blend exhibited the highest retention of approximately 59%, whereas RR0 showed a retention of 50%. This suggests that the presence of reclaimed rubber, which contains carbon black and crosslinked gel precursors, enhances the thermal stability of the rubber matrix, thereby retarding degradation better than virgin NR alone. However, for oil-swollen aging, all blends showed a significant reduction in tensile strength, with retention values dropping below 20%. This drastic decrease is attributed to the non-polar nature of natural rubber, which readily absorbs non-polar oil, leading to severe swelling and the disruption of physical entanglements, regardless of RR content.

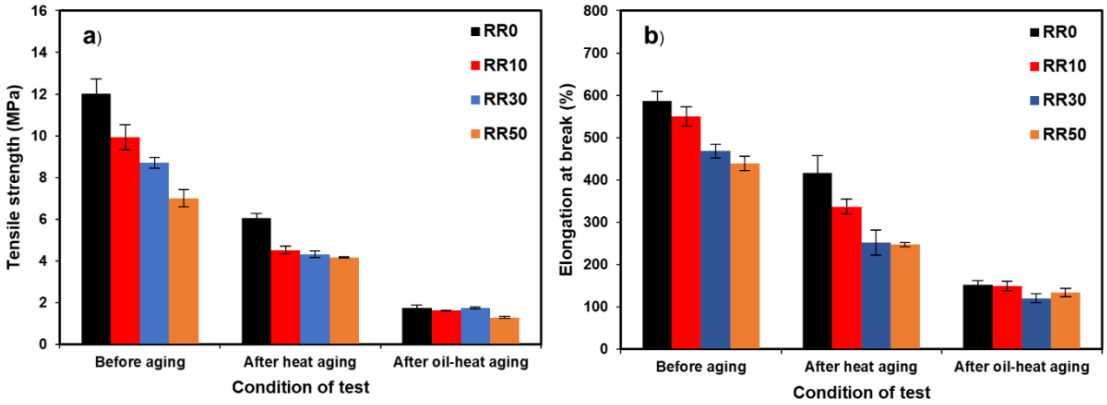

Figure 3. Tensile properties of NR/RR Blend at ratios of 100/0, 90/10, 70/30, and 50/50, including a) Tensile strength and b) Elongation at break.

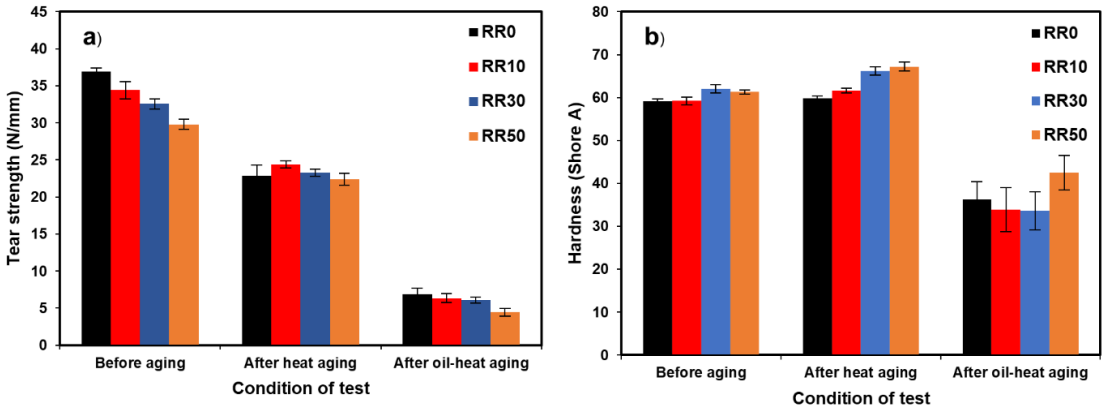

Figure 4. a) Tear strength and b) Hardness of NR/RR Blend at ratios of 100/0, 90/10, 70/30, and 50/50.

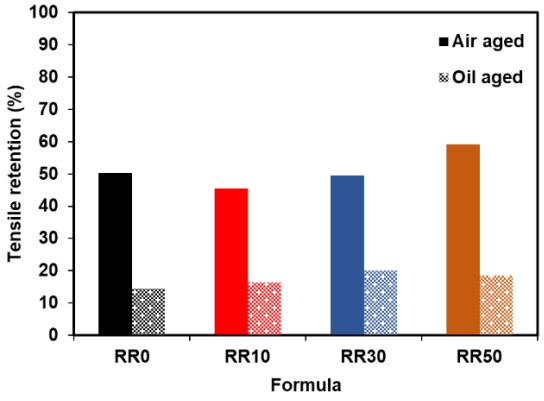

Figure 5. Percentage retention of tensile strength for NR/RR blends after thermal aging (100 °C, 7 days) and oil-swollen aging (100 °C, 7 days).

3.4 Thermal stability

Thermogravimetric analysis (TGA) measures the change in mass of a sample and its rate (velocity) of change in response to temperature or time in a controlled environment. This technique is primarily used to assess the thermal and oxidative stabilities of materials, as well as their compositional properties. The thermal decomposition behavior of NR/RR blends is shown in Figure 6. The decomposition temperatures at different weight losses and various stages are also summarized in Table 3. The initial slight weight loss observed around 180–200 °C was attributed to volatile substances, such as stearic acid, and to adsorbed water around 300 °C [22]. The main degradation process of the blends began at approximately 330 °C and was completed around 450 °C. This decomposition was due to the breakdown of NR segments, as evidenced by the major peak observed in the DTG curve. The degradation of NR is particularly sensitive to the presence of oxidized structures and the depletion of sulfur crosslinks. Notably, the decomposition temperatures at 5, 10, 20, and 30% weight loss for the blends were higher as the RR content increased. This increase in thermal stability is attributed to two factors: the physical shielding effect of carbon black and inorganic fillers in the reclaimed rubber, which acts as a thermal barrier, and the presence of thermally stable mono- and di-sulfidic crosslinks (C-S-C, C-S_2-C) generated during the reclaiming process, which possess higher bond dissociation energy than the polysulfidic bonds predominant in virgin NR. The char residue obtained for both blends at the final temperature exhibited behavior that was essentially the same as a function of the RR phase concentration. As noted, the RR composition was analyzed by TGA before formulating the rubber ingredients. So, the rubber, hydrocarbon, and filler content were controlled. This has led to the unchanged residue remaining in the rubber formulations.

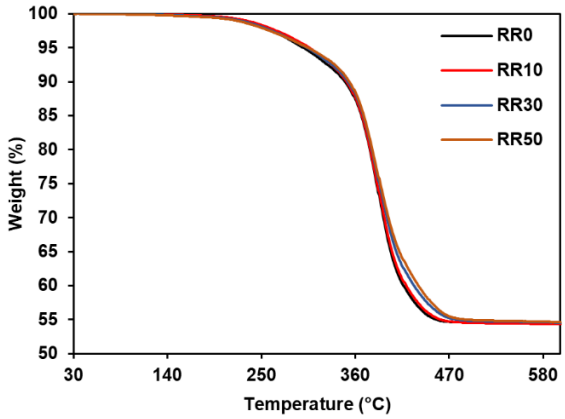

Figure 6. TGA of NR/RR blends at ratios of 100/0, 90/10, 70/30, and 50/50 at a heating rate of 15 °C/min.

Table 3. Temperature at 5%, 10%, 20% and 30% weight loss and char residue of NR/RR blend.

Sample	Decomposition temperature (°C)				Char residue (%)
	T-5%	T-10%	T-20%	T-30%	
RR0	298.5	348	376.5	392.25	54.3070
RR10	306	349.5	377.25	393	54.3077
RR30	303	351	378.75	396.75	54.5472
RR50	304.5	353.25	379.5	398.25	54.6205

3.5 Activation energy

Figure 7 shows the thermogram of the blends at various heating rates. A lower heating rate caused faster degradation of the rubber. This is simply due to the time the resident spends degrading the rubber. A longer time has led to faster chain scission due to its heat storage, resulting in faster decomposition. The data from Figure 7 were utilized to determine the activation energy (Ea) according to Equation (6) by graphing ln(β) versus 1000/T for conversion rates that ranged from 0.05 to 0.45, in increments of 0.05. The outcomes are presented in Figure 8. It was then computed into activation energy using the OFW, KAS, and FRD methods. A comparison of activation energy (Ea) values obtained from the OFW, KAS, and FRD methods is shown in

Figure 9. The Ea is higher for RR0 because of its virgin rubber. Higher Ea indicates that more energy is required to break the specific bonds in the rubber molecules. The activation energy trends across all approaches exhibit strong consistency, with smooth, stable curves indicating negligible variation. This consistency validates the precision and dependability of the computed activation energies [23, 24].

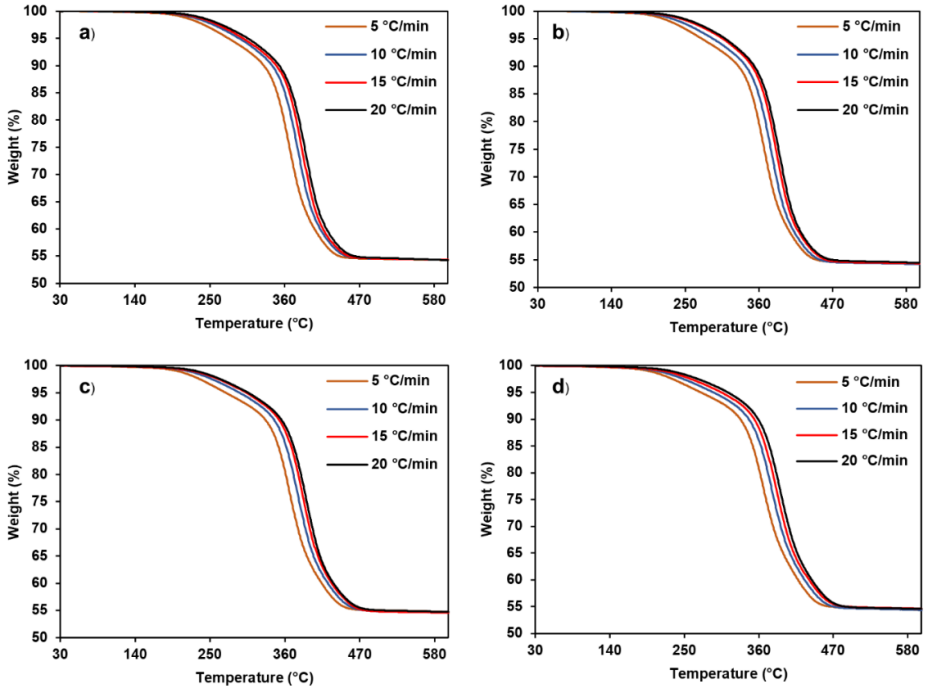

Figure 7. Thermogravimetric analysis (TGA) of NR/RR blends with ratios of a) 100/0, b) 90/10, c) 70/30, and d) 50/50 was conducted at heating rates of 5, 10, 15, and 20 °C/min. The analysis was performed in the temperature range of 30–600 °C under a nitrogen atmosphere.

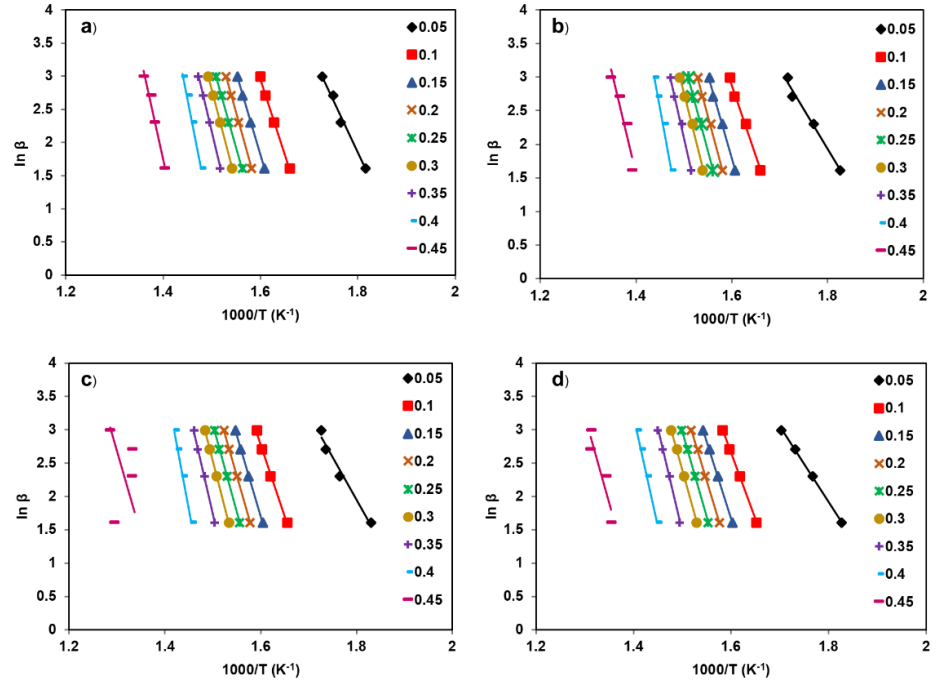

Figure 8. Plot derived from TGA curves at various conversion rates (0.05–0.45) for NR/RR blends with ratios of a) 100/0, b) 90/10, c) 70/30, and d) 50/50 using the Ozawa–Flynn–Wall (OFW) method.

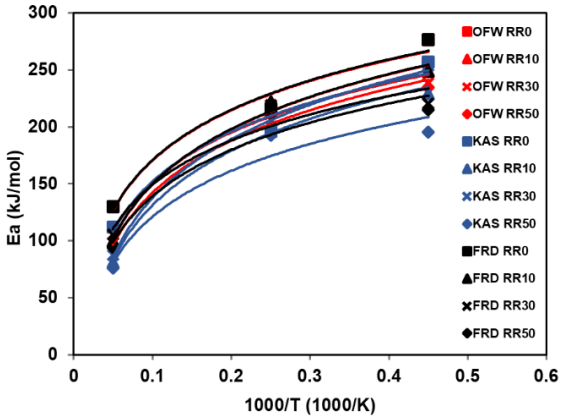

Figure 9. The activation energy relationships of RR0 (rectangle), RR10 (triangle), RR30 (cross), and RR50 (square) as a function of the transformation extent obtained by the OFW method (red symbols), KAS method blue symbols), and FRD method (black symbols) applied to the thermal decomposition.

3.6 Lifetime prediction of NR/RR blends

As shown in Table 4, the high correlation coefficients ($R^2 > 0.97$) obtained from the linear regression of the OFW plots further confirm the reliability of the kinetic data at this conversion level. Additionally, a heating rate of 20 °C/min was employed as the reference condition to simulate a rigorous thermal history, ensuring that the predicted service life provides a conservative estimate under accelerated thermal stress.

Table 4. Kinetic parameters used for lifetime prediction based on the OFW method at the failure criterion ($\alpha = 0.05$).

Sample	Linear Equation (y = mx + c)	Correlation Coefficient (R^2)	Activation Energy (E_a) [kJ/mol]
RR0	y = -15.649x + 30.015	0.9882	130.10
RR10	y = -11.934x + 23.412	0.9854	99.32
RR30	y = -12.685x + 24.786	0.9759	105.46
RR50	y = -11.308x + 22.271	0.9993	94.01

Predicting a material's lifetime is essential for accident prevention and for ensuring optimal product performance by mitigating premature degradation. For the lifetime calculation, the kinetic parameters were determined at a conversion degree of 0.05, consistent with the methodology reported by [15]. This specific conversion level was selected as the failure criterion because it corresponds to the onset of the degradation process. Although a 5% mass loss may appear minimal, in practice, such a degree of chemical change can lead to a significant degradation in the material's mechanical properties. Therefore, lifetime prediction at this threshold is essential for accurately assessing the material's durability and safety in real-world applications. The lifetime was computed using Equation (7) with the acquired data and the previously calculated activation energy. Figure 10 shows the predicted lifetime of NR/RR blends with ratios of 100/0, 70/30, and 50/50, respectively. The results show a persistent reduction in lifetime as temperatures increase. For example, as the temperature increases from 70 °C to 100 °C, the lifetime of RR0 decreases from 195 years to 5.15 years, RR10 lifetime decreases from 3.77 years to 0.24 years, RR30 lifetime decreases from 7.65 years to 0.40 years, and RR50 lifetime decreases from 2.01 years to 0.15 years. Temperature significantly affects the durability of rubber due to the direct relationship between activation energy and temperature. The RR composition substantially affects the lifetime [16]. At lower temperatures, such as 30 °C, increased RR content results in shorter lifetimes. This behavior is attributed to the presence of shortened molecular chains and pre-oxidized structures in the reclaimed rubber, which accelerate degradation kinetics. Conversely, at elevated temperatures, specifically above 250 °C, blends with higher RR content show extended lifetimes due to a crossover phenomenon. This behavior is attributed to the dominance of stable monosulfidic and disulfidic crosslinks and to the physical shielding effect of carbon black, which enhances thermal stability in the later phases [25]. It should be noted

that the lifetime predicted in this study (e.g., >195 years at 70 °C) represents a theoretical thermal lifetime under an inert nitrogen atmosphere. In real-world service conditions, rubber products are simultaneously exposed to oxygen, ozone, UV radiation, and mechanical stress, which significantly accelerate degradation. Therefore, the actual service life will be considerably shorter than the TGA-based predictions. However, this method remains valuable for comparing the relative thermal stability of different rubber formulations under controlled thermal stress.

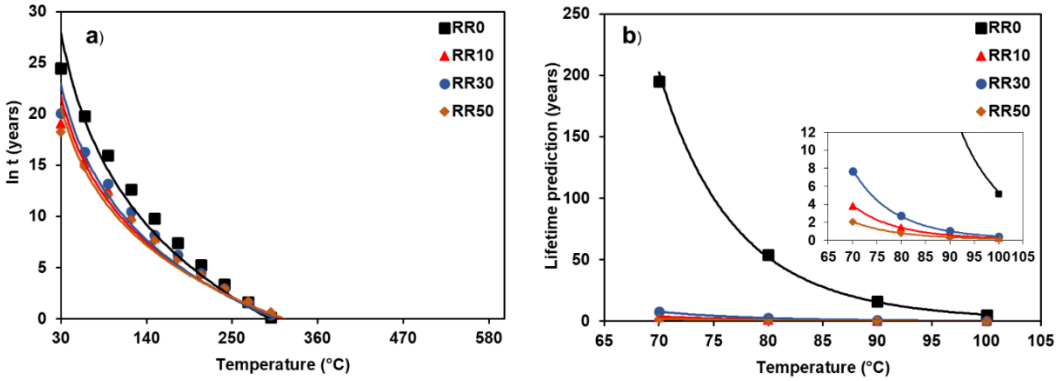

Figure 10. OFW lifetime prediction curves of NR/RR blends at ratios of (RR0) 100/0, (RR10) 90/10, (RR30) 70/30, and (RR50) 50/50: (a) prediction over the full temperature range, and (b) expanded view at 70–100 °C. (Calculated with a heating rate of 5 °C/min at conversion α = 0.05).

4. Conclusions

The experimental results showed that the mechanical properties of NR/RR blends tended to decrease continuously with increasing amounts of reclaimed rubber due to the decreasing molecular weight of the RR due to chain break during the reclaiming process and the inhomogeneity of the phases in the NR/RR blends, resulting in a decrease in the mechanical properties of NR upon the addition of reclaimed rubber. However, the hardness increased due to the remaining filler in the reclaimed rubber. The thermal degradation of NR/RR blends was studied using TGA. The obtained experimental TGA data were used to calculate the activation energy (Ea) using the Ozawa–Flynn–Wall (OFW) Method. It was found that vulcanized rubber without RR addition had the highest activation energy, due to its natural origin. The results showed that NR/RR blends at all ratios had slightly lower lifetimes than NR vulcanized in the temperature range of 30-600 °C and at a service temperature of 70 °C. When comparing the NR/RR blends at different ratios, the values ranged from 195 years to 2.01 years. This indicates that the addition of RR may affect the service life of the products. The results of this study provide useful information and a foundation for rubber compounders when using RR in their formulations.

5. Acknowledgements

We gratefully acknowledge the financial support from Prince of Songkla University, Pattani Campus, through Grant No. SAT6703029S. The first author wishes to thank the Faculty of Science and Technology, Prince of Songkla University, Pattani Campus, for providing a personal scholarship under Grant No. 013/2566.

Author Contributions:

- **Conceptualization** – Nabil Hayeemasae; Weerawut Naebpetch
- **Methodology** – Nabil Hayeemasae; Weerawut Naebpetch; Sitisaiyidah Saiwari
- **Software** – NA
- **Validation –** Nabil Hayeemasae; Weerawut Naebpetch; Sitisaiyidah Saiwari
- **Formal analysis** – Sutiwat Thumrat
- **Investigation** – Sutiwat Thumrat
- **Resources** – Nabil Hayeemasae; Weerawut Naebpetch
- **Data curation** – Sutiwat Thumrat; Nabil Hayeemasae

- **Writing – original draft preparation** – Sutiwat Thumrat; Nabil Hayeemasae
- **Writing – review & editing** – Nabil Hayeemasae
- **Visualization** – Nabil Hayeemasae; Weerawut Naebpetch; Sitisaiyidah Saiwari
- **Supervision** – Nabil Hayeemasae; Weerawut Naebpetch; Sitisaiyidah Saiwari
- **Project administration** – Nabil Hayeemasae
- **Funding acquisition** – Nabil Hayeemasae

Funding: This research was funded by Prince of Songkla University, Pattani Campus, grant number SAT6703029S, and the APC was funded by the same grant.

Conflicts of Interest: The authors declare no conflict of interest.

References

[1] Formela, K. Waste tire rubber-based materials: Processing, performance properties and development strategies. *Adv. Ind. Eng. Polym. Res.* **2022**, *5*(4), 234–247. https://doi.org/10.1016/j.aiepr.2022.06.003

[2] [2] Ali, F.; Denis, R. Waste Rubber Recycling: A Review on the Evolution and Properties of Thermoplastic Elastomers. *Materials* **2020**, *13*(3), 782. https://doi.org/10.3390/ma13030782

[3] Daniele, R.; Andrea, D. Novel uses of recycled rubber in civil applications. *Adv. Ind. Eng. Polym. Res.* **2022**, *5*(4), 214–233. https://doi.org/10.1016/j.aiepr.2022.08.005

[4] Pranay, G.; Sukhanand, S. B.; Rohit, S.; Praful, S.; Ajay, G. D. Use of waste rubber tyre in construction of bituminous road. *Int. Res. J. Mod. Eng. Technol. Sci.* **2023**, https://doi.org/10.56726/irjmets44098

[5] Dennis, G. The value of different recycling technologies for waste rubber tires in the circular economy—A review. *Front. Sustain.* **2024**, https://doi.org/10.3389/frsus.2023.1282805

[6] Said, S.; Lucía, A.; Morena, R. M.; Nourredine, A. H. Thermo-mechanical devulcanization and recycling of rubber industry waste. *Resour. Conserv. Recycl.* **2019**, *144*, 180–186. https://doi.org/10.1016/j.resconrec.2019.01.047

[7] Zhao, X.; Hu, H.; Zhang, D.; Zhang, Z.; Peng, S.; Sun, Y. Curing behaviors, mechanical properties, dynamic mechanical analysis and morphologies of natural rubber vulcanizates containing reclaimed rubber. *e-Polymers* **2019**, *19*(1), 482–488. https://doi.org/10.1515/epoly-2019-0051

[8] Darestani, F. T.; Bakhshandeh, G. R.; Abtahi, M. Mechanical and Viscoelastic properties of natural rubber/reclaimed rubber blends. *Polym. Bull.* **2006**, *56*(4-5), 495–505. https://doi.org/10.1007/s00289-006-0508-4

[9] Aditya, R.; Pranav, K. S.; Prashant, P.; Nimisha, R. S. Minimization and Utilization of Byproduct. *Int. J. Innov. Eng. Sci.* **2023**, *8*(5), https://doi.org/10.46335/IJIES.2023.8.5.8

[10] Mishel, P. F.; Steffi, P. F.; Vijayalakshmi, S. Conventional and modern waste treatment approaches – bioremediation of rubber waste. In *Sustainable Bio-Remediation of Waste Rubber*, Elsevier: **2023**; pp 97–113. https://doi.org/10.1016/B978-0-443-15206-1.00007-4

[11] Tao, Z.; Lucia, A.; Michel, G.; Nourredine, A. H. An overview on waste rubber recycling by microwave devulcanization. *J. Environ. Manage.* **2024**, *353*, 120122. https://doi.org/10.1016/j.jenvman.2024.120122

[12] Woo, C. S.; Park, H. S. Useful lifetime prediction of rubber component. *Eng. Fail. Anal.* **2011**, *18*(7), 1645–1651. https://doi.org/10.1016/j.engfailanal.2011.01.003

[13] Núñez, L.; Villanueva, M.; Núñez, M. R.; Rial, B. Lifetime prediction of the epoxy system DGEBA (n= 0)/1, 2-DCH modified with an epoxy reactive diluent by thermogravimetric analysis. *J. Appl. Polym. Sci.* **2003**, *89*(14), 3835–3839. https://doi.org /10.1002/app.12536

[14] Viorel, S.; Orsina, V.; Alexandru, P. The estimation of thermal endurance for some heteropoly acidic catalysts from thermogravimetric decomposition data. *J. Therm. Anal. Calorim.* **2017**, *127*(1), 273–282. https://doi.org/10.1007/s10973-016-5479-6

[15] Ngudsuntear, K.; Limtrakul, S.; Vatanatham, T.; Arayapranee, W. Mechanical and aging properties of hydrogenated epoxidized natural rubber and its lifetime prediction. *ACS Omega* **2022**, *7*(41), 36448–36456. https://doi.org/10.1021/acsomega.2c04225

[16] Ahn, W.; Lee, J. M.; Lee, H. S. A Study on Life Time Prediction of ACM Rubber Composite Using Accelerated Test and Thermogravimetric Analysis. *Elastomers Compos.* **2014**, *49*(2), 144–148. https://doi.org/10.7473/EC.2014.49.2.144

[17] Toop, D. Theory of Life Testing and Use of Thermogravimetric Analysis to Predict the Thermal Life of Wire Enamels. *IEEE Trans. Electr. Insul.* **1971**, *EI-6*(1), 2–14. https://doi.org/10.1109/TEI.1971.299128

[18] Plota, A.; Masek, A. Lifetime Prediction Methods for Degradable Polymeric Materials—A Short Review. *Materials* **2020**, *13*(20), 4507. https://doi.org/10.3390/ma13204507

[19] Saiwari, S.; Lohyi, E.; Nakason, C. Application of NR Gloves Reclaim: Cure and Mechanical Properties of NR/Reclaim Rubber Blends. *Adv. Mater. Res.* **2013**, *844*, 437–440. https://doi.org/10.4028/www.scientific.net/AMR.844.437

[20] https://doi.org/Thitithammawong, A.; Hayichelaeh, C.; Nakason, W.; Jehvoh, N. The use of reclaimed rubber from waste tires for production of dynamically cured natural rubber/reclaimed rubber/polypropylene blends: Effect of reclaimed rubber loading. *J. Met. Mater. Miner.* **2019**, *29* (2), 85–94. https://doi.org/10.14456/jmmm.2019.24

[21] Candau, N.; Chazeau, L.; Chenal, J. M.; Gauthier, C.; Ferreira, J.; Munch, E.; Thiaudière, D. Strain induced crystallization and melting of natural rubber during dynamic cycles. *Phys. Chem. Chem. Phys.* **2015**, *17*(23), 15331–15338. https://doi.org/10.1039/C5CP00384A

[22] Lu, L.; Lu, L.; Cai, J.; Frost, R. L. Desorption of stearic acid upon surfactant adsorbed montmorillonite: A thermogravimetric study. *J. Therm. Anal. Calorim.* **2010**, *100*(1), 141–144. https://doi.org/10.1007/s10973-009-0169-2

[23] Ammineni, S. P.; Nagaraju, C.; Lingaraju, D. Thermal degradation of naturally aged NBR with time and temperature. *Mater. Res. Express* **2022**, *9*(6), 065305. https://doi.org/10.1088/2053-1591/ac7302

[24] Mohit, A.; Remya, N. Pyrolysis characteristics and kinetics study of native polyculture microalgae using thermogravimetric analysis. *Biomass Convers. Biorefin.* **2024**, *14*(16), 19825–19833. https://doi.org/10.1007/s13399-023-04175-z

[25] Joseph, A. M.; George, B.; Alex, R. Effect of devulcanization on crosslink density and crosslink distribution of carbon black filled natural rubber vulcanizates. *Rubber Chem. Technol.* **2016**, *89*(4), 653–670. https://doi.org/10.5254/rct.16.84819